P8R.7 REAL-TIME CALCULATION OF HORIZONTAL WINDS USING MULTIPLE DOPPLER RADARS: A NEW WDSS-II MODULE

Arthur Witt[1]*, Rodger A. Brown[1] and V. Lakshmanan[1,2]

[1]NOAA/National Severe Storms Laboratory, Norman, Oklahoma
[2]CIMMS/University of Oklahoma, Norman, Oklahoma

1. INTRODUCTION

As part of NSSL's new emphasis on multi-radar/multi-sensor analysis techniques for real-time applications (Stumpf et al. 2004), this project set out to extend NSSL's Warning Decision Support System - Integrated Information (WDSS-II; Hondl 2003) to include a multi-Doppler capability for the calculation of the 3D wind field in regions of observed radial velocity data. To allow for maximum flexibility, in terms of the number of radars used as input sources, the "overdetermined dual-Doppler" analysis method (Kessinger et al. 1987) was selected for implementation as a new module in the multi-radar portion of WDSS-II. For a user-specified analysis domain, the multi-Doppler module calculates the three wind components (*u*, *v* and *w*) in regions where two or more Doppler radars are providing valid radial velocity measurements. The module generates output files of each wind component, along with a horizontal vector field (*u* and *v* combined), which are displayable via WDSS-II (e.g., Fig. 1).

2. ANALYSIS METHOD

The first step involves "mapping" the input radial velocity data to a 3D latitude-longitude-height grid. This entails going through all the grid points one by one, and assigning information from nearby radial data for each radar. After the analysis domain and grid spacing have been set (typical grid spacings are 0.01° x 0.01° x 1 km or 0.005° x 0.005° x 0.5 km), the radial velocity data are partially "scale-filtered" to match the horizontal grid spacing. This involves using a running average along each radial, with the number of sample volumes (gates) used to calculate an average value roughly equal, in total length, to the horizontal grid spacing. Then, at each grid point, the closest elevation scans above and below the grid point are identified, and the radial gates nearest to the grid point on both elevation scans are located. The vertical distance between the grid point and each elevation angle is determined, and this information is saved, along with the radial velocity values. If a grid point is below the lowest elevation scan or above the highest elevation scan for a particular radar, then the vertical distance to the closest elevation angle is determined. If this distance is less than one radar beamwidth, then the radial gate nearest to the grid point on this elevation scan is located, and the vertical distance and radial velocity value are saved. The vertical distance (between a grid point and radial gate) is used to calculate an "elevation-weight" for the radial velocity value, which will be used in calculating the 3D wind field. For grid points with elevation scans above and below them, the elevation-weight is the vertical distance between the radial gate and the grid point divided by the larger of: 1) the vertical distance between the elevation angles above and below the grid point or, 2) the beamwidth. For example, if a grid point is located exactly halfway between adjacent elevation angles, and the distance between these elevation angles is larger than the beamwidth, then elevation-weight = 0.5. For grid points below the lowest elevation scan or above the highest elevation scan, elevation-weight is the vertical distance between the radial gate and the grid point divided by the beamwidth.

The time period of radial velocity data used in the mapping process is specified by the user, and is usually set to the volume scan update interval. If this time interval is greater than the volume scan update rate for one or more radars, then radial velocity data from previous volume scans may be included, and used in the multi-Doppler calculations. Similarly, if any elevation angles are repeated within a volume scan, such as is the case with the Terminal Doppler Weather Radar (TDWR), those additional elevation scans are also included in the mapping process. Hence, it is possible for some grid points to have more than one radial velocity value for a given elevation angle. Ultimately, multiple radial velocity values from the same radar that have been assigned to a grid point are combined into a single value.

*Corresponding author address: Arthur Witt, NSSL, 1313 Halley Circle, Norman, OK 73069. E-mail: Arthur.Witt@noaa.gov

After all the points in the full 3D grid have been mapped, the 3D wind field is calculated. For a particular grid point, "valid" radial velocity data are needed from two or more radars. The definition here for valid velocity data is one or more non-missing radial velocity value with an elevation-weight of at least 0.5. If this condition is met, and more than one non-missing radial velocity value for a particular radar has been mapped to the grid point, these multiple values are combined into a single weighted average value (using elevation-weight). If data are available from only two radars, then an additional criterion is that the difference in viewing angle (azimuth) between the two radars for that grid point be at least 20°.

For the grid points meeting these criteria, the values of u, v and w are calculated using the overdetermined dual-Doppler analysis method presented by Kessinger et al. (1987). For a radial velocity value V_i observed at (x, y, z) by a radar located at (x_i, y_i, z_i), the u and v components of the wind field are

$$u = \frac{[\sum R_i V_i (x - x_i)]S_{yy} - [\sum R_i V_i (y - y_i)]S_{xy} + [w + V_t][S_{xy}S_{yz} - S_{yy}S_{xz}]}{S_{xx}S_{yy} - (S_{xy})^2} \quad (1)$$

$$v = \frac{[\sum R_i V_i (y - y_i)]S_{xx} - [\sum R_i V_i (x - x_i)]S_{xy} + [w + V_t][S_{xy}S_{xz} - S_{xx}S_{yz}]}{S_{xx}S_{yy} - (S_{xy})^2} \quad (2)$$

where R_i is the range to the observation and

$S_{xx} = \sum (x - x_i)^2$
$S_{yy} = \sum (y - y_i)^2$
$S_{xy} = \sum (x - x_i)(y - y_i)$
$S_{xz} = \sum (x - x_i)(z - z_i)$
$S_{yz} = \sum (y - y_i)(z - z_i)$;

V_t is the terminal velocity (Rogers 1964; Foote and duToit 1969) of raindrops, and is estimated from the equivalent radar reflectivity factor (Z_e)

$$V_t = -3.8(\rho_0/\rho)^{0.4} Z_e^{0.0714} \quad (3)$$

where ρ is the air density at the height of the observation, and ρ_0 is the air density at sea level. All summations are performed over the number of radars providing velocity data.

Vertical velocity is determined via the mass continuity equation

$$\frac{\partial u}{\partial x} + \frac{\partial v}{\partial y} + \frac{\partial w}{\partial z} = \kappa w \quad (4)$$

where κ is the logarithmic change in air density with height. Assuming a standard atmosphere, $\kappa \cong 0.1$ km^{-1}. Since Eqs. 1, 2 and 4 are all functions of u, v and w, an iterative process is used to determine the final values of u, v and w (Brown et al. 1981). The process starts at the top of the analysis domain, and proceeds downward. At each horizontal level, w is initially specified and u and v are computed from Eqs. 1 and 2 based on that value. Then w is estimated from Eq. 4 using values of u, v and w from both the current and previous horizontal levels (using data from two horizontal levels is necessary because of the vertical derivative in Eq. 4). Specifically, at horizontal level i

$$w_i = w_{i+1} - \left(\overline{\frac{\partial u}{\partial x} + \frac{\partial v}{\partial y}} - \kappa w \right) \Delta z \quad (5)$$

where the overbar represents the average of values at levels i and $i+1$. After this new value of w is determined, the process is repeated, until either u, v and w have all stabilized (defined as a Δw between iterations of <0.1 m s^{-1}) or the maximum number of iterations allowed has been reached.

3. TEST RESULTS

The new multi-Doppler module was tested (in simulated real-time) on data from two severe weather events. The primary test case was 12 June 2002 (21:01 UTC – 23:47 UTC), where data from four WSR-88Ds [KICT (Wichita, KS), KVNX (Vance Air Force Base, OK), KTLX (Oklahoma City, OK) and KINX (Tulsa, OK)] were available (Fig. 2). Another reason for selecting this case as the focus of testing was that the analysis domain was located ~180° from KICT and ~85° from KVNX (which makes comparing the radial velocity

data with the *u* and *v* components of the wind field a simple task). The second test case was 8 May 2003 (22:01 UTC – 22:45 UTC), where data from the Oklahoma City (OKC) TDWR and KTLX WSR-88D were available for a tornadic supercell that moved across the OKC metro area (Fig. 3).

Even though data from four radars were available for the 12 June case, the initial test run was done using data from just KICT and KVNX, because these were the two closest radars, and, because of the viewing angles (relative to the analysis domain), this would allow for a more direct comparison of the *u* and *v* fields with the radial velocity data. Evaluation of the 3D wind fields for this test run showed generally good agreement between the *u* field and the radial velocity data from KVNX, and the *v* field and the radial velocity data from KICT. Unfortunately, the *w* field quickly developed large errors, with absolute values of *w* often >50 m s^{-1}, and occasionally >100 m s^{-1}. There was also generally no organized pattern in the *w* field, with sharp gradients common. And because of the iterative process involved in the calculation of *u*, *v* and *w*, these large errors with *w* led to errors in *u* and *v* (although the impact was generally <5 m s^{-1}). Since the main operational use of the multi-Doppler output is expected to involve the horizontal wind field versus the vertical velocity, a second version of the module was created that just calculates the *u* and *v* components (by using Eqs. 1 - 3 with *w* set to zero). Test results for this 2D horizontal-wind module (on the same data from KICT and KVNX) showed very good agreement between the *u* and *v* fields and the radial velocity data. Given the superior performance of the 2D module in determining the horizontal wind field, all subsequent testing focused on this version.

Two additional dual-Doppler test runs were made for the 12 June case using data from KICT/KINX and KVNX/KTLX, to investigate the effects of using data from more distant radars. Compared to the KICT/KVNX run, some data coverage was lost at the lowest grid levels (due to both greater heights for the lowest elevation scan for KINX and KTLX, and larger areas affected by range folding). Also, significant storm-scale features in the wind field were less well-defined (e.g., Fig. 4). For the KICT/KINX run, the velocity data from KINX had numerous problems with dealiasing errors, which led to corresponding errors in the horizontal wind field. However, despite these problems, even when data at far ranges (i.e., >200 km) were used, if the data quality was generally good (i.e., no dealiasing errors or noisy data), then the horizontal wind field also looked good (for larger-scale features).

A final test run for the 12 June case was done using data from all four radars. Compared to the KICT/KVNX run, there was greater areal coverage in the horizontal wind field, mainly over KVNX (in the cone-of-silence region) and along the baseline of KICT/KVNX (because of the 20° minimum viewing angle requirement when only two radars are used) (e.g., Fig. 5). However, the data tended to be somewhat noisier in these regions, compared to areas where both KICT and KVNX contributed radial velocity data to the calculations. As with the dual-Doppler test runs that used data from KINX or KTLX, significant storm-scale features in the wind field were less well-defined, although not to the same extent. Also, with more radars providing radial velocity data, there was an increase in dealiasing errors corrupting the wind field calculations (e.g., Fig. 6).

The 8 May test case was significantly different from the 12 June case in that the analysis domain was confined to a relatively small area close to both radars, due to the short baseline distance (19 km) between the radars (which limits the area where calculations can be made). Because of the close proximity of the storm to both radars, and the top elevation angles to which both radars scan, radial velocity data were available for only about the lower half of the storm. Despite this limitation, the 8 May case does offer the opportunity to make estimates of the near-surface (<1 km AGL) wind field, which was not possible for the 12 June case (due to the greater distance of the radars). Test results for the 8 May case were similar to those from the 12 June case, with very good agreement between the *u* and *v* fields and the radial velocity data. In addition to the direct comparisons to the radial velocity data, overlays of the horizontal vector plots with the lowest-elevation-angle reflectivity data match what conceptual models of the air flow in a supercell storm would suggest (Fig. 7). The 8 May case also demonstrates a problem involving the use of the full 3D-wind module on operational radar data – that data coverage may not extend through the entire depth of the storm of interest, which would not allow for proper calculation of the *w* field. This is another factor favoring use of the 2D horizontal-wind module versus the full 3D-wind module.

4. SUMMARY

Two new multi-Doppler modules have been developed for NSSL's real-time WDSS-II,

based on the "overdetermined dual-Doppler" analysis method. One module calculates the full 3D wind field, whereas the other calculates just the 2D horizontal wind. Initial testing of the 3D-wind module showed major problems with the *w* field, which also caused errors in the horizontal wind field. This led to the development of the second module, which produced superior test results for the horizontal wind field. Although the modules can handle data from more than two radars, results from the primary test case indicate that it may be better to only use data from the two closest radars. Including data from more distant radars can "wash-out" significant air flow signatures (Fig. 5), as well as increase the probability of corrupting the calculations with dealiasing errors (Fig. 6). Further testing is needed to more completely resolve this issue, since greater areal coverage is obtained by using data from as many radars as possible. The best approach may involve extending the modules to utilize data from all available radars, but make assessments at individual grid points on which data to use from specific radars. In any case, optimizing the quality of the input radar data (by minimizing dealiasing errors and noisy data) is crucial to obtaining a good wind-field calculation. Although data from only two severe weather events were evaluated for this project, these initial results are very encouraging, and suggest that a promising new capability for measuring the 2D wind field in real-time has been added to WDSS-II.

5. ACKNOWLEDGMENTS

The authors thank Don Burgess and Travis Smith for reviewing the manuscript. This project was supported by the Federal Aviation Administration under FAA contract DTFA03-01-X-90007.

6. REFERENCES

Brown, R. A., C. R. Safford, S. P. Nelson, D. W. Burgess, W. C. Bumgarner, M. L. Weible, and L. C. Fortner, 1981: Multiple Doppler radar analysis of severe thunderstorms: Designing a general analysis system. NOAA Tech. Memo. ERL NSSL-92.

Foote, G. B., and P. S. duToit, 1969: Terminal velocity of raindrops aloft. *J. Appl. Meteor.,* **8,** 249-253.

Hondl, K. D., 2003: Capabilities and components of the Warning Decision Support System – Integrated Information (WDSS-II). Preprints, *19th Intl. Conf. on Interactive Information and Processing Systems (IIPS),* Long Beach, CA, Amer. Meteor. Soc., CD-ROM.

Kessinger, C. J., P. S. Ray, and C. E. Hane, 1987: The Oklahoma squall line of 19 May 1977. Part I: A multiple Doppler analysis of convective and stratiform structure. *J. Atmos. Sci.,* **44,** 2840-2864.

Rogers, R. R., 1964: An extension of the Z-R relation for Doppler radar. Preprints, *11th Weather Radar Conf.,* Boston, MA, Amer. Meteor. Soc., 158-161.

Stumpf, G. J., T. M. Smith, V. Lakshmanan, K. L. Manross, and K. D. Hondl, 2004: Status of Multiple-Sensor Severe Weather Application Development at NSSL. Preprints, *20th Intl. Conf. on Interactive Information and Processing Systems (IIPS) for Meteor., Oceanography, and Hydrology,* Seattle, WA, Amer. Meteor. Soc., CD-ROM.

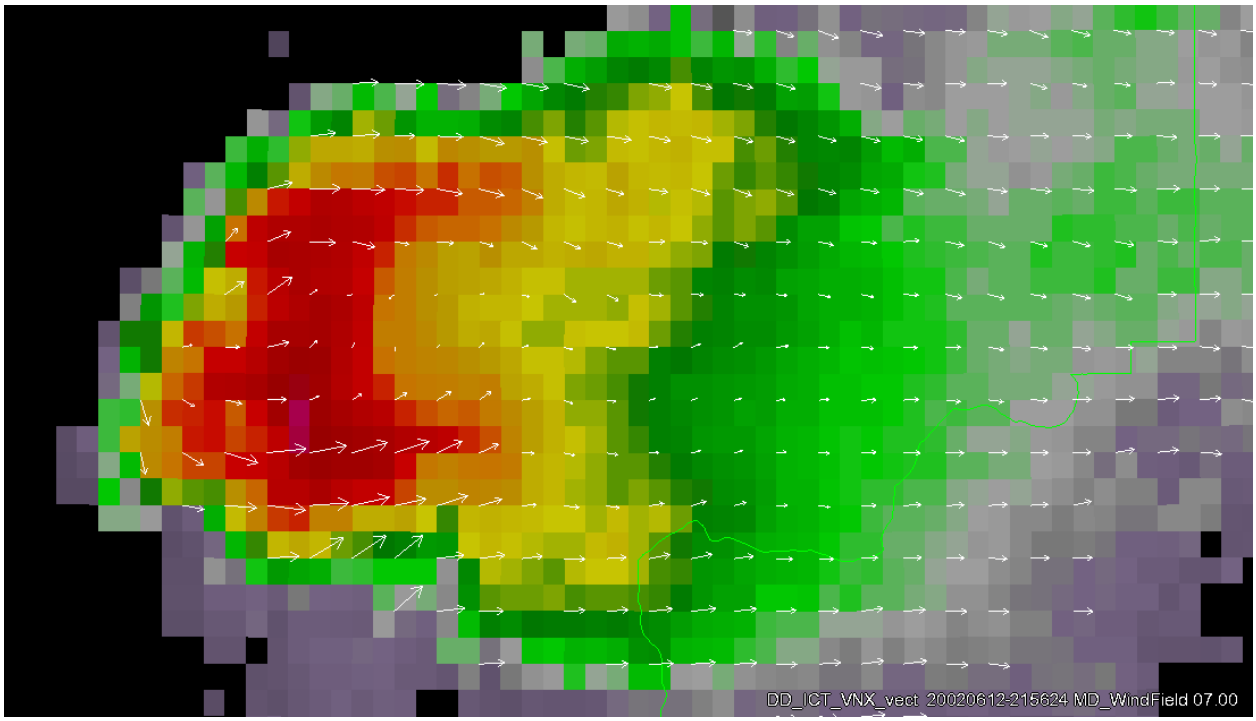

Fig. 1. Example of output (horizontal wind field) from the multi-Doppler module. Data are from two WSR-88Ds (KICT and KVNX) for a height of 7 km MSL. Analysis time is 21:56 UTC on 12 June 2002. The storm centroid is located at an azimuth/range of 168°/99 km from KICT and 87°/83 km from KVNX.

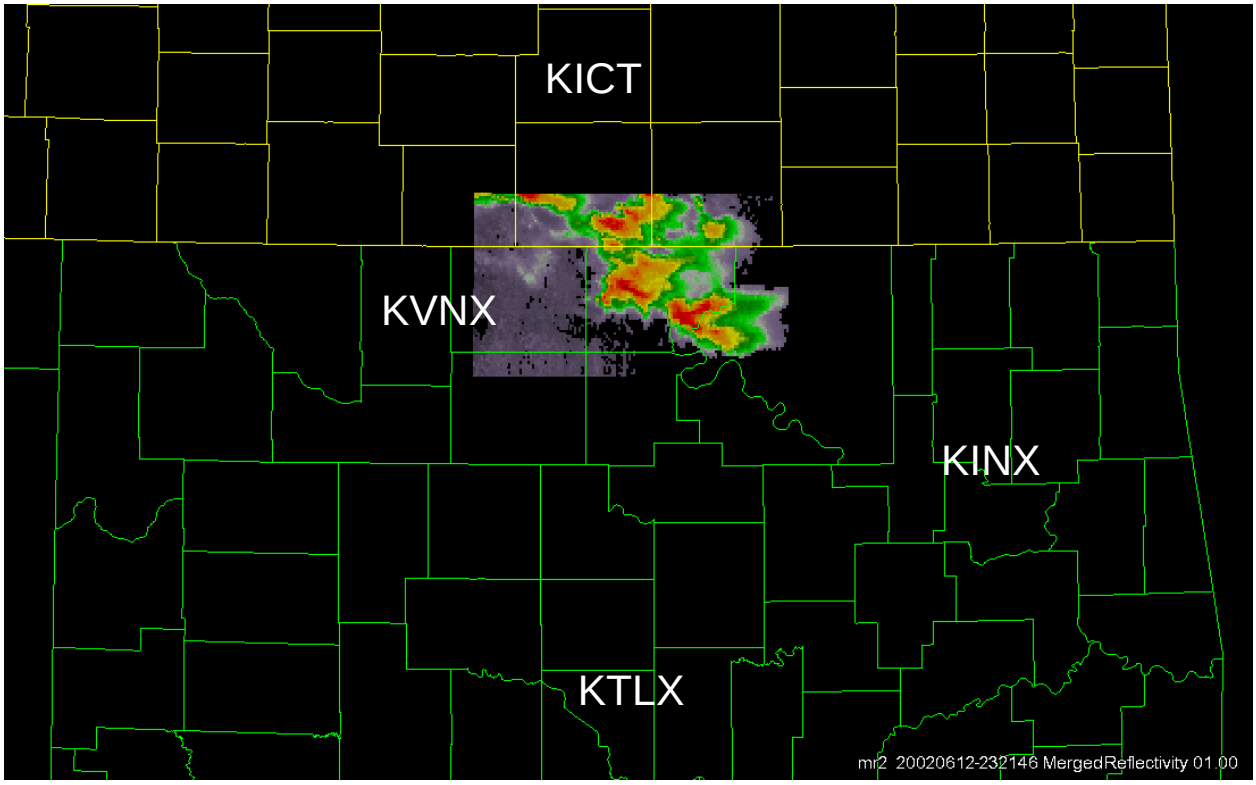

Fig. 2. Analysis domain for the 12 June 2002 test case. The grid spacing is 0.01° x 0.01° x 1 km. Reflectivity image shown is a composite of data from all four radars, and is from 23:21:46 UTC at a height of 1 km MSL. Radar locations are indicated via their four letter abbreviations.

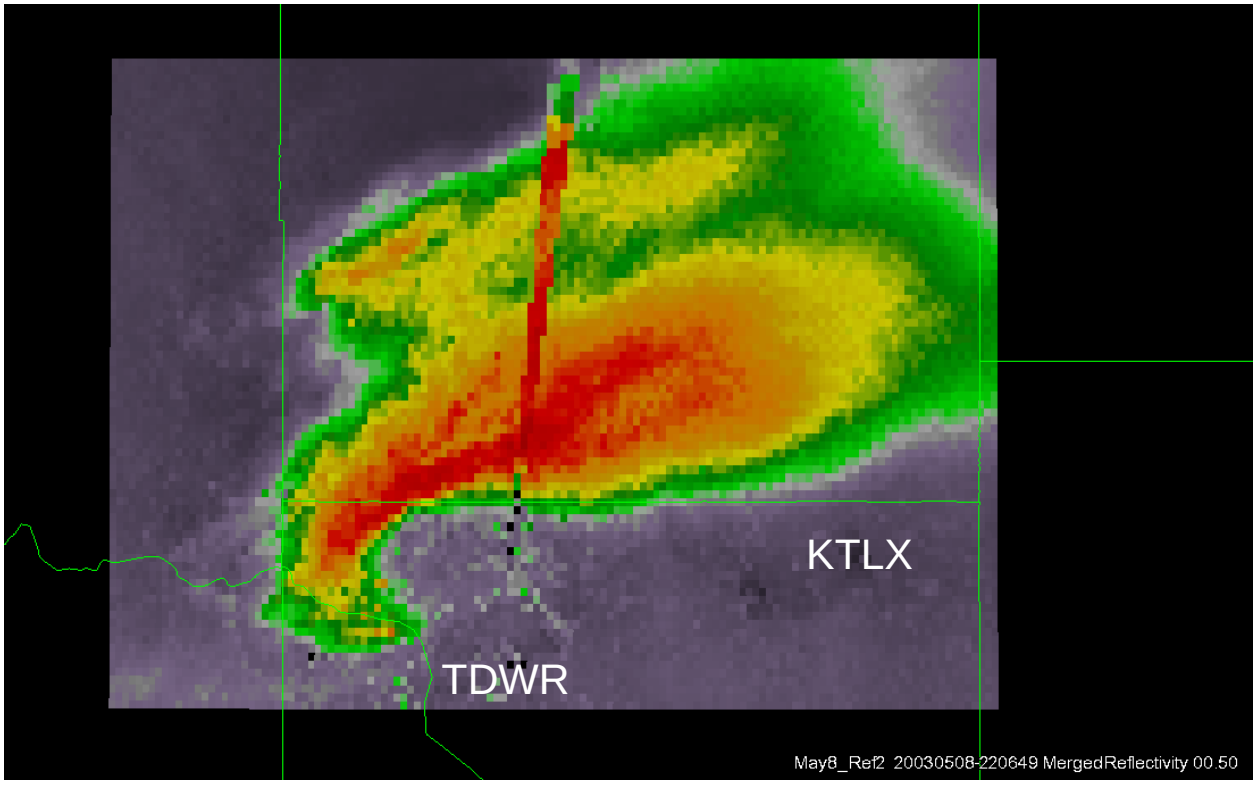

Fig. 3. Analysis domain for the 8 May 2003 test case. The grid spacing is 0.005° x 0.005° x 0.5 km. Reflectivity image shown is a composite of data from KTLX and TDWR, and is from 22:06:49 UTC at a height of 0.5 km MSL. The anomalous radials (extending from TDWR at ~6° azimuth) are due to beam blockage of the TDWR, with reflectivity data only being used from KTLX.

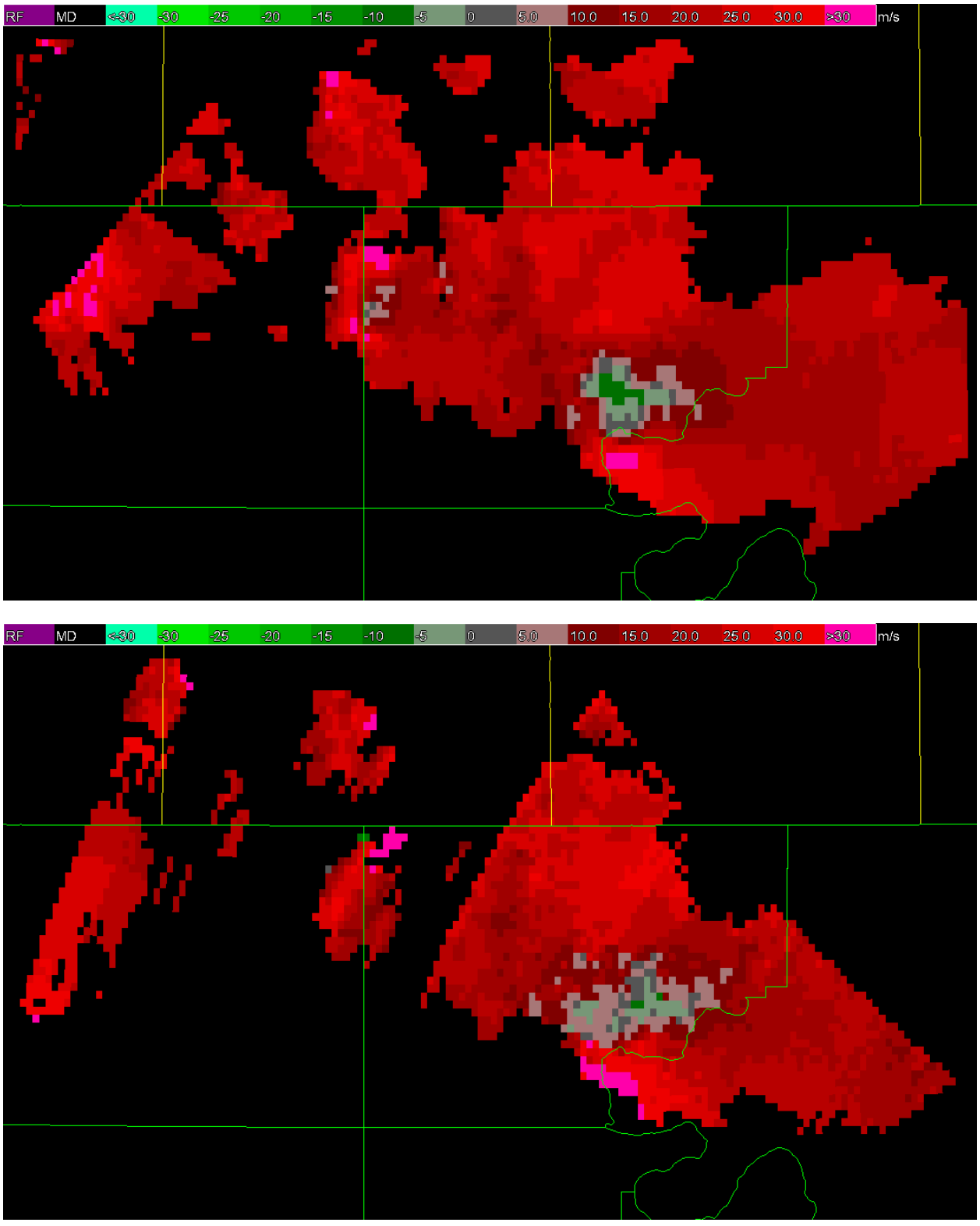

Fig. 4. *U* component for the KICT/KVNX run (top) and KICT/KINX run (bottom) at 22:40 UTC at a height of 7 km MSL.

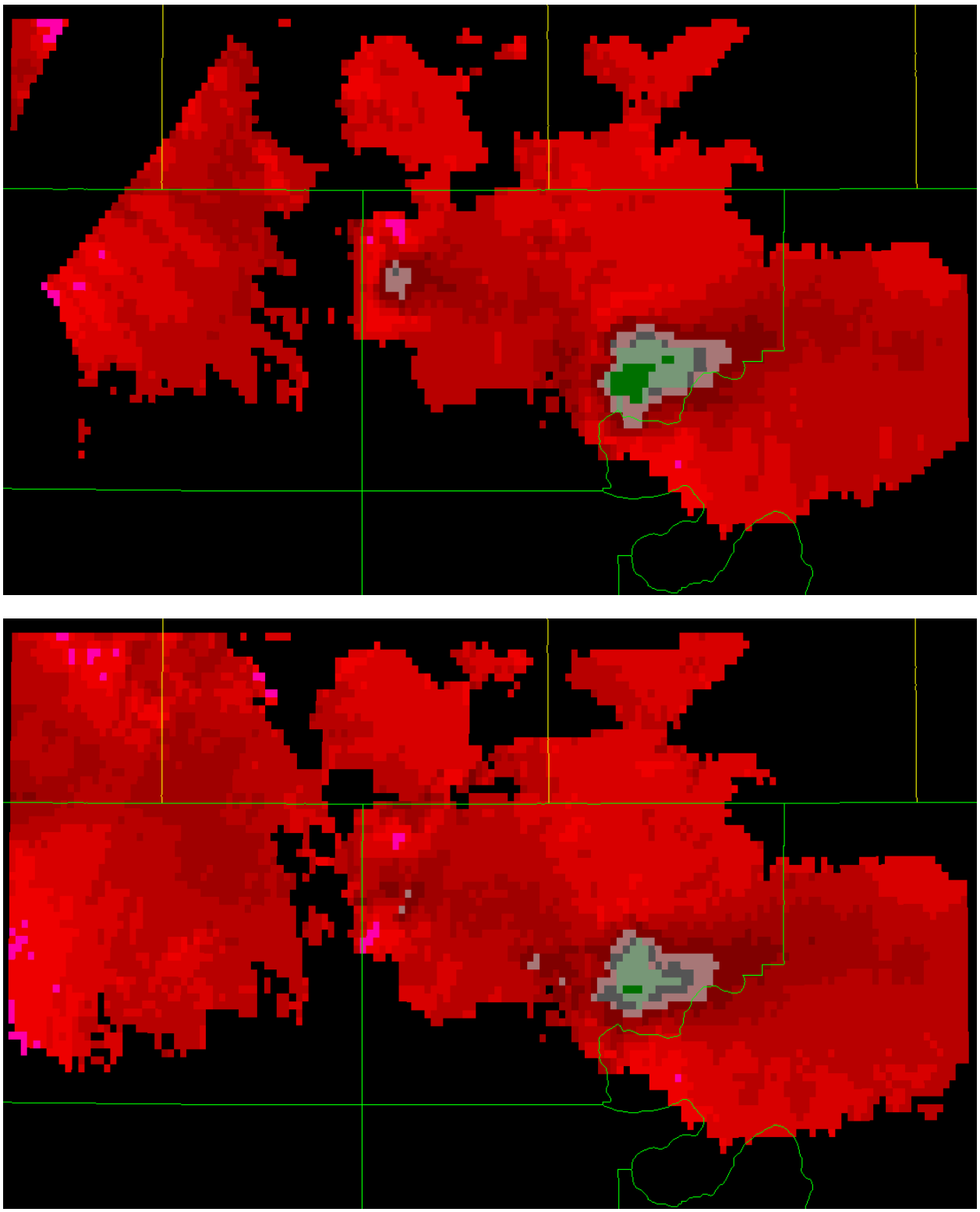

Fig. 5. *U* component for the KICT/KVNX run (top) and the four-radar run (bottom) at 22:45 UTC at a height of 8 km MSL.

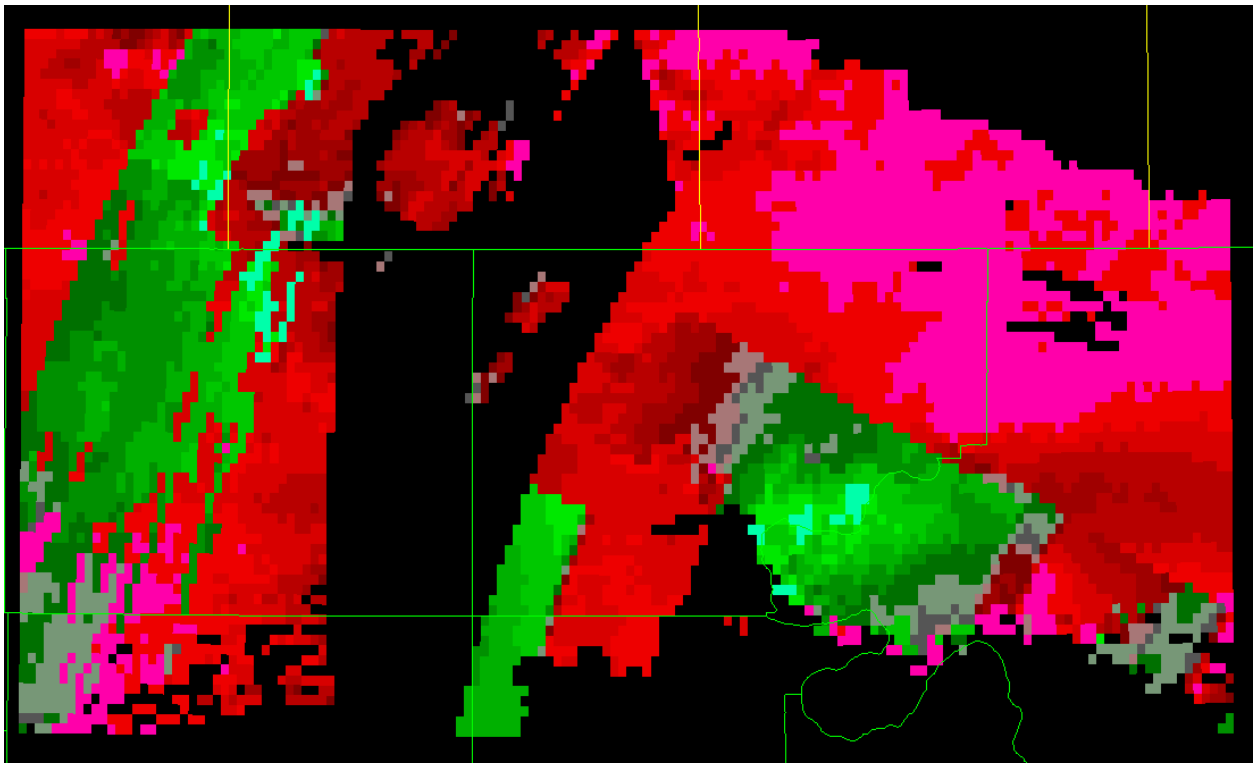

Fig. 6. *U* component for the four-radar run at 23:05 UTC at a height of 12 km MSL, illustrating the problems caused by velocity dealiasing errors (from KINX). At this particular time, data were unavailable from KVNX (leading to the region of missing data along the KICT/KTLX baseline).

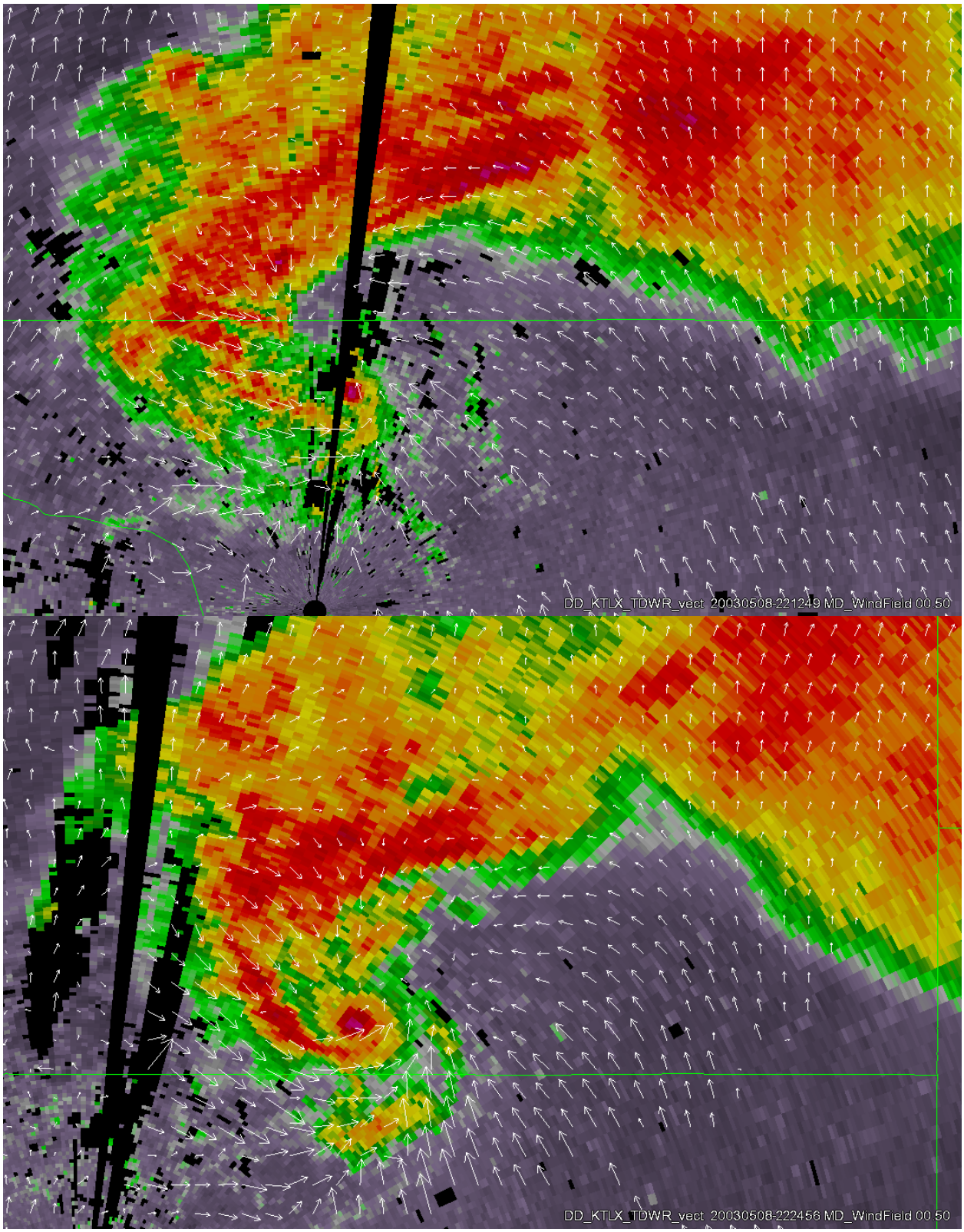

Fig. 7. Reflectivity data from the OKC TDWR (elevation angle 0.5°) with corresponding 2D horizontal wind field (at 0.5 km MSL or ~0.2 km AGL) at 22:13 UTC (top) and 22:25 UTC (bottom).